This is a preprint, the final version is subject to change, of the American Mineralogist (MSA)
Cite as Authors (Year) Title. American Mineralogist, in press.
(DOI will not work until issue is live.) DOI: http://dx.doi.org/10.2138/am.2013.4217

Revision 1

Hydration properties of synthetic high-charge micas saturated with different cations: An experimental approach

ESPERANZA PAVÓN[1], MIGUEL A. CASTRO[2], MOISÉS NARANJO[2], M. MAR ORTA[2], M. CAROLINA PAZOS[2] AND MARÍA D. ALBA[2*]

[1]Unité de Catalyse et de Chimie du Solide, UCCS. CNRS, UMR8181, Université Lille Nord de France .59655 Villeneuve d'Ascq, France

[2]Instituto Ciencia de Materiales de Sevilla (CSIC-Universidad de Sevilla) Avda. Américo Vespucio, 49. 41092 Sevilla, Spain

ABSTRACT

An understanding of the interaction mechanisms between exchangeable cations and layered silicates is of interest from both a basic and an applied point of view. Among 2:1 phyllosilicates, a new family of swelling high-charge synthetic micas has been shown to be potentially useful as decontaminant. However, the location of the interlayer cations, their acidity and the water structure in the interlayer space of these silicates are still unknown. The aim of this paper was therefore to study the hydration state of the interlayer cations in the interlayer space of high-charge expandable micas and to evaluate the effect that this hydration has on the swelling and acidity behavior of these new materials. To achieve these objectives, three synthetic micas with different with different charge density total layer charges (ranging between 2 and 4 per unit cell) and with five interlayer cations (Na^+, Li^+, K^+, Mg^{2+} and Al^{3+}) were synthesized and their hydration state, interlayer space, and acidity analyzed by DTA/TG, XRD, and ^1H MAS NMR spectroscopy. The results showed that the hydration state depends on both the layer charge and the nature of the interlayer cation. A high participation of the

* *Corresponding author: E-mail: alba@icmse.csic.es*

inner-sphere complexes in the highly charged confined space has been inferred and proposed to induce Brönsted acidity in the solid.

Keywords. Swelling, synthetic micas, Brönsted acidity, hydration, inner sphere, DTA, XRD and NMR

INTRODUCTION

Confined waters are ubiquitous in nature and they play important roles in geological, biological and technical processes (Wang et al., 2003). Water under confinement shows different behaviors from the bulk due to the influences from the limiting boundaries and this has received great attention (Dysthe and Wogelius, 2006). 2:1 type phyllosilicates are widely distribute in soils and sediments and they contain considerable confined waters in their interlayer pores (Grim, 1962; Bergaya et al., 2006). Therefore, the interlayer space of swelling 2:1 clays plays an important role in geochemical, environmental, and industrial processes (Grim, 1962; Odom, 1984; Van Olphen, 1984; Murray, 1986; Colin et al., 1997; Murray, 1999; Murray, 2000; Hensen et al., 2001). In light of this, an understanding of the interaction mechanisms between exchangeable cations and layered silicates is of interest from both a basic and an applied point of view. Thus, it is important to determine both the physicochemical properties of these materials (Sposito et al., 1999) and how the hydration of interlayer cations and the clay surface controls the swelling, dispersion, and ion-exchange properties of these layered silicates as these factors have an important influence on their use in catalytic reactions, adsorption, and waste disposal, amongst others (Laszlo, 1986; Adams, 1987; Sposito, 1989; Michalopoulo et al., 1995).

The swelling properties of clays have been studied extensively, both experimentally (Weiss et al., 1990; Cases et al., 1992; Bérend et al., 1995; Michot et al., 2002; Ferrage et al., 2005; Rinnert et al., 2005; Trausch et al., 2006; Salles et al., 2008) and theoretically (Boek et

al., 1995a,b; de Siqueira et al., 1997; Young and Smith, 2000; Hensen et al., 2001; Hensen and Smit, 2002; Whitley and Smith, 2004; Tambach et al., 2004; Liu and Lu, 2006; Smith et al., 2006; Tambach et al., 2006) and are now relatively well understood. Mooney et al. (1952a,b) were among the first authors to show that smectites are able to sorb up to half their mass in water and that the water sorption behavior is strongly dependent on the nature of the exchangeable cation. The mechanisms underlying these interactions have since been the subject of several reviews (Sposito and Prost, 1982) and has been explained by a number of arguments: the size of hydrated cations (Shainberg and Kemper, 1967; Gast, 1969; Gast, 1992*)*, their ability to lose a water molecule at the clay surface, thus forming a stronger inner-sphere complex (Eisenmann, 1962; Maes and Cremers, 1978), their hydration state in the interlayer (Laird and Shang, 1997) or their polarizability that influences the formation of surface complexes (Shainberg and Kemper, 1967; Sposito, 1984; Maes and Cremers, 1986). Therefore, the equilibrium water density of such hydrated clays depends on the type of clay mineral, the type of interlayer counterion, the applied pressure and temperature, and the water vapor pressure (Grim, 1962; Slade et al., 1991; Sato et al., 1992).

The negative layer charge in 2:1 clays is balanced by exchangeable counterions such as Na^{+}, K^{+}, and Ca^{+2}. In broad terms, it is the tendency of these interlayer counterions to solvate that causes the clays to expand in the presence of water and other polar solvents (Hendricks et al., 1940; Balek et al., 2006; Balek et al., 2008). Thus, all known smectites show a rational series of 00l reflections at medium relative humidities. Under these conditions, the basal (d_{001}) spacing of the sodium form is 1.66–1.72 nm after solvation with ethylene glycol (Srodon, 1980). At low humidity, some Na^{+}-smectites may display characteristics of vermiculite (d_{001}=1.45 nm), whereas the Ca^{2+}-exchanged forms retain their smectitic character. The expansion of vermiculite is more restricted because its layer charge is higher than that of smectite and is largely located in the tetrahedral sheet (Srodon, 2006).

Moreover, Harward et al. (1969) observed that the swelling capacity of smectite and vermiculite not only depends on the amount of layer charge but also is related to their source.

Although swelling 2:1 layered silicates have traditionally been considered to be those containing a total layer charge of between 0.4 and 1.8 per unit cell (smectite and vermiculite groups), a new family of synthetic swelling silicates with tuned layer charge values of between 2.0 and 4.0 per unit cell has recently been synthesized (Gregorkiewitz and Rausell-Colom, 1987; Park et al., 2002; Komarneni et al, 2005) and a general synthetic method reported (Alba et al., 2006). These swelling high-charge micas, in which the layer charge can be adjusted, could be highly valuable for the decontamination of harmful divalent and heavy metal cations (Ravella et al., 2008) via ion-exchange reactions and for the selective removal of highly radioactive ions (Alba et al., 2006) and hydrocarbon molecules (Alba et al., 2011).

The location of the interlayer cation and the water structure in the interlayer space of high-charged micas are likely to affect the properties that make them relevant in several applied fields. In those high charged synthetic micas, the layers bear a high permanent negative charge compensated by counterions located between them (interlayer space). These counterions are the origin of two interesting features: mica swelling and ionic exchange. The former refers to the entrance of water into the interlayer, while the latter involves the replacement of original counterions Na^+ in the mica interlayer by other ions initially in the aqueous solution in contact with the mineral, and the concomitant release of Na^+ in the solution (Slabaugh, 1954; Barrer et al., 1963; Martin and Laudelout, 1963; Fripiat et al., 1964; Robeyns et al., 1971; Maes and Cremers, 1978; Ewin et al., 1981; Dyer et al., 2000). Both processes will be strongly influenced by the location in a confined space with a high electric field of the interlayer cation. Knowledge of the hydration state of the interlayer cations in these materials is, therefore, vital for environmental protection applications. Moreover, water molecules in interlayer space of clay minerals can donate protons and thus serve as the major

Brönsted acid sites in the interlayer regions (Bergaya et al., 2006) and unsaturated ‘‘broken’’ bonds at the edge can coordinate unsaturated interlayer cations which behave as Lewis acid sites (Lambert and Poncelet, 1997).

The 2-D environments alter the properties of confined waters from many aspects. (1) The hard clay layers physically limit the mobility of waters on the direction perpendicular to the basal surfaces. (2) The oxygen atoms on basal surfaces interact with interlayer waters via H-bonding. The clay layer charges polarize the waters to a large extent and thus impose effects on their interactions with surfaces. (3) Some counterions form strong chemical bonds with waters and thus rigid hydration shells. Thus, all those aspects will modify the acidity of the mica (Criscenti and Sverjensky, 1999)

In light of this, the aims of this work were to study the hydration state of the cations in the interlayer space of highly charged swelling micas, to analyze the properties of these cations that affect their hydration state in a confined space with a high electric field, and to evaluate the effects that this hydration may have on the swelling behavior and acidity of these new materials. To achieve these objectives, three synthetic micas with different total layer charges and five different interlayer cations were selected. In order to study the influence of ionic radius on the hydration state, three alkali metal cations (Li^+, Na^+, and K^+) were selected. The electric parameter (q/r) effect was analyzed using three cations from the third period of the periodic table (Na^+, Mg^{+2}, and Al^{+3}). The layer charge of the silicate was also analyzed using three highly charged micas with layer charges of between 2 and 4.

EXPERIMENTAL METHODS

Synthesis

A procedure similar to that described by Alba et al. (2006) was employed. Near-stoichiometric powder mixtures with the molar compositions (8 - *n*) SiO_2, (*n*/2) Al_2O_3, 6 MgF_2, and (2*n*) NaCl were used to synthesize Na-Mica-*n* (*n* = 2, 3, 4). The starting materials were SiO_2 from Sigma (CAS no. 112945-52-5, 99.8% purity), $Al(OH)_3$ from Riedel-de Haën (CAS no. 21645-51-2, 99% purity), MgF_2 from Aldrich (CAS no. 20831-0, 98% purity), and NaCl from Panreac (CAS no. 131659, 99.5% purity). All reagents were mixed and ground vigorously before heating up to 900 °C in a Pt crucible for 15 h. After cooling, the solids were washed with deionized water and dried at room temperature. The as-synthesized samples are named Na-Mica-*n* (*n* ranging between 2 and 4).

Cation-Exchange Process

The as-synthesized Na-Mica-n were exchanged with solutions of Li^+, K^+, Mg^{+2} and Al^{+3} salts at concentrations that ensured the molar amount of cation was 10 times the cation-exchange capacity (CEC) of the mica (Miller et al., 1982). The most important characteristics of these ions in solution are displayed in Table 1 (Rayner-Canham, 2000). The reagents used were $MgCl_2$ from Sigma-Aldrich (CAS n° 7786-30-6, 99.99% purity), KCl from Fluka (CAS n° 7447-40-7, >99% purity), $AlCl_3$ from Fluka (CAS n° 7784-13-6, >99.0 % purity), and LiCl from Fluka (CAS n° 7447-41-8, >99.0% purity). Ion-exchange was carried out by mixing 30 mL of the aqueous salt solutions with 2 g of the Na-Mica-*n* (*n*=2, 3 and 4) then shaking the resulting suspension in a magnetic stirrer at room temperature. After 8 h, the suspension was filtered through an 8 μm filter and this process repeated three more times. The resulting solids were subsequently washed three times by shaking in distilled water for 6 h, then dried at room temperature and analyzed by XRD to evaluate the purity of the samples under the conditions reported in the experimental section. These solids are referred to as *X*-Mica-*n* where X=Na^+, Li^+, K^+, Mg^{+2}, or Al^{+3} and *n*=2, 3, or 4.

Sample Characterization.

Simultaneous DTA/TG (differential thermal analysis/ thermogravimetry) measurements were performed at the ICMS (CSIC-University of Seville, Spain) using a TA (SDT-Q600) instrument equipped with a Pt/Pt-Rh thermocouple for direct measurement of the temperature at the sample/reference crucible from room temperature up to 300°C (heating rate: 10°C min^{-1}), in air. Approximately 150 mg of sample was used, and the DTA reference was pure aluminum oxide.

X-ray diffraction (XRD) patterns were obtained at the CITIUS X-ray laboratory (University of Seville, Spain) using a Bruker D8 Advance instrument equipped with a Cu K_α radiation source operating at 40 kV and 40 mA. The powder XRD patterns were obtained, at the relative humidity of the lab ca. 55 %, in the 2θ-range 3–70° with a step size of 0.05° and a time step of 1° 2θ/min. The patterns for oriented water aggregates were recorded to determine the maximum swelling state of all the silicates at room temperature. These patterns were measured in the 2θ range 1-20°, with a time step of 4 s and a step size of 0.02°, without a monochromator but with a Ni filter.

^{1}H (SP) MAS-NMR spectra were recorded at the Spectroscopy Service of ICMS (CSIC-US, Seville, Spain) using a Bruker DRX400 spectrometer equipped with a multinuclear probe. Powdered samples were packed in 4-mm zirconia rotors and spun at 10 kHz. ^{1}H MAS spectra were obtained using a typical π/2 pulse-width of 4.1 μs and a pulse space of 5 s. The chemical shift values are reported in ppm with respect to tetramethylsilane.

RESULTS AND DISCUSSION

DTA/TG

The DTA analysis show several endothermic peaks between 25 and 300°C, with the number of peaks and their temperatures depending on the mica layer charge and the interlayer cation (Suppl. 1). Table 2 shows the temperature of the main endothermic peaks observed in DTA and the number of water molecules per unit cell calculated from the TG curves. The coordination number of the water coordination sphere of each cation in the X-Mica-*n* is illustrated in Figure 1.

The influence of the ionic radius of the interlayer cation was analyzed for the mica samples exchanged with alkali-metal cations. Only one endothermic peak (between 60 and 85°C), which corresponds to those water molecules less strongly bonded to the silicate structure and located in the basal planes of the unit cell, was observed for an *n* value of 4 (Hendrcks and Jefferson, 1938; Grim, 1942). The number of water molecules per unit cell (ca. 3) is slightly lower than that observed for smectites or vermiculite (ca. 4) (Black et al., 2008). When $n<4$, the DTA curves for the Na^+- and K^+-exchanged samples did not suffer any change and the temperature for the endothermic peak remained in the range described above. However, the Li-Mica-*n* ($n=2$ and 3) showed different endothermic peaks at higher temperatures (ca. 150°C) that may reveal water molecules bound to the structure with different strengths. The number of water molecules per cation is plotted versus the ionic radius of these three cations in Figure 1a. It can be seen from this figure that the number of water molecules per cation decreases as the ionic radius increases. It is well known that the q/r factor (as measure of the amount of charge by size unit) decreases, and, therefore, their hydration capacity decreases, as the ionic radius increases (Rayner-Canham, 2000). Thus, the extremely low values obtained for the number of water molecules per cation are likely to be due to an interaction between the interlayer cations and the negative electrostatic force of the layers that decreases the effective charge of the cation and, therefore, its q/r factor. This effect is higher as the layer charge increases.

The influence of the electrostatic parameter (q/r) and the number of water molecules per cation on the DTA curves of exchanged mica with polyvalent cations was analyzed using the X-Mica-*n* samples exchanged with Na^{+}, Mg^{+2}, and Al^{+3} cations. The DTA curves for an *n* value of 4 showed an endothermic peak between 60 and 85°C, whereas a new endothermic peak was observed at higher temperature (ca. 140°C) for the sample exchanged with aluminum. Al^{3+} is a small cation with a high polarizing effect; therefore the hydration water of the cations in the interlayer space may form H-bonds with the clay-oxygen plane, which is favored as negative charge in the oxygen basal plane increases (Yariv, 1992). When the layer charge decreases, complex DTA curves are observed for Mg^{+2} and Al^{+3} micas, with endothermic peaks at higher temperature (between 90°C and nearly 200°C). This suggests that water molecules with different bonding energies coexist in the interlayer space of these silicates. Although the number of water molecules per cation increases with the charge of the cations for X-Mica-3 and X-Mica-2; this relationship is not observed for the highest charged mica, X-Mica-4. The number of water molecules per cation in these cases is found to be proportional to the increase of the q/r factor for these cations (Figure 1b), with the increase being higher for the smallest layer charge (*n*=2).

Studies undertaken in montmorillonites suggest that the amount of interlayer water depends on the hydration energy of the adsorbed cations and on hydration of the surface. Thus, it was noted that the ion is more important than the interlayer surface for most divalent cations (Mg^{+2} or Ca^{+2}), whereas the influence of the layered surface on hydration predominates for larger divalent and monovalent cations (Mackenzie, 1964). The water-bonding energy in the interlayer space of Mg-vermiculites mainly depends on the interlayer cation and shows similar DTA curves despite differences in the chemical composition of the tetrahedral and octahedral sheets (Justo et al., 1993).

The DTA/TG results reported herein suggest a double influence for swelling high-charge micas whereby the incorporation of water molecules into the interlayer space of highly charged micas is determined by the effective q/r factor of the cation, which in turn is influenced by both the layer charge of the silicate and by the ionic radius of the inorganic cation (alkali-metal cations) or the electrostatic factor (third period cations). In this respect, Glasser et al. (1960) have shown that polyvalent ions tend to detach themselves from the silicate surface and become incorporated into the water layers.

XRD

The XRD patterns of samples with the highest layer charge (n=4) and exchanged with alkali-metal cations (Figure 2) show a unique 001 reflection corresponding to a basal spacing of around 12.0 Å, which is characteristic of a single monolayer of water in the interlayer space of swelling silicates (Alba et al., 2001), as inferred by the water content determined by TGA. The basal spacing for Na^+- and K^+-exchanged micas remains constant as the layer charge decreases, whereas a single new reflection corresponding to a more hydrated state of the mica appears for the Li^+-exchanged sample for a layer charge of three or two. These findings are consistent with the number of water molecules obtained in the previous section: the calculated number of water molecules is approximately 2.7 and 2.4 for Na^+ and K^+ regardless of the layer charge of the silicate (Figure 1a), thus implying a constant d_{001} distance for the layers. In the case of Li^+, the number of water molecules increases as the layer charge decreases, probably due to the shift to higher *d* values observed in the 001 XRD pattern for this silicate. Hensen et al. (2001) have reported that the degree of clay hydration at low water pressures is governed by the type of counterion, with Li-montmorillonite having the highest water content. The 001 reflection for the X-Mica-4 exchanged with Mg^{+2} and Al^{+3} show the main peak at around 12.0 Å and 13.5 Å, respectively. The Mg-Mica-4 shows an additional

small peak at 13.5 Å. When the layer charge decreases, the position of the 001 reflection for the Mg^{+2}- and Al^{+3}-exchanged samples shifts to a lower 2θ value, which corresponds to higher basal space (up to 14.0 Å). This increased layer separation for the mica is likely to be due to the fact that small cations are located in two layers closer to the surface whereas larger ones primarily reside in the midplane (Hensen et al., 2001). This means that more water molecules can be adsorbed in the former case, thus resulting in the higher clay water contents observed by TG analysis.

These findings suggest that X-Mica-*n* layer swelling is controlled by the balance between the repulsive forces between adjacent 2:1 layers and the attractive forces between hydrated interlayer cations and the negatively charged surface of these 2:1 layers, as previously observed for smectites (Norrish, 1954; Kittrick, 1969). Thus, when Al^{3+}-for-Si^{4+} substitutions occur in tetrahedral sites in montmorillonite-like layers, the charge deficit is distributed amongst the three nearest neighbor basal oxygen atoms, which are strongly under-saturated and produce strong attractive interactions with interlayer cations. This strong local under-saturation is sometimes assumed to decrease layer hydration (Laird, 1996; Laird, 1999). However, previously reported experimental results are not consistent with this expected influence of the size and location of the layer charge on hydration behavior. For example, Sato et al. (1992) reported similar d_{001} values for smectite with different layer-charge locations, and smaller d_{001} values were not observed for smectites with a higher layer charge. Furthermore, Chiou and Rutherford (1997) and Michot et al. (2005) reported an increase in H_2O content with increasing layer charge. Similar results were obtained by Laird (1999), who attributed the increased hydration to H_2O adsorption on the external surfaces of the crystallites. However, this has a limit because the attractive forces between the hydrated interlayer cation and the 2:1 layers increases, and the interlayer thickness decreases, at high layer charge (Ferrage et al., 2005; Melkior et al. 2009). Moreover, steric effect has to be

considered because a d_{001} value of 12.0 Å implies an estimated interlayer space height of 2.6 Å (d_{001}-9.4 Å). If we take into account that the Van der Waal diameter of water molecule is 2.82 Å (Finney, 2001), them, there is steric effect to accommodate the fully hydrated cations (ranging between 4 and 2 cations per unit cell) at the middle of the interlayer space. Therefore, the partial insertion of the cations in the hexagonal holes is necessary and the cations are partially coordinated by basal oxygens of the tetrahedral sheet, in good agreement with the low amount of water molecules observed by TG.

The XRD data presented herein show that both the radius (r) and the charge (q) of the cations affect the hydration state of the mica. Thus, when the q/r ratio for the interlayer cations is less than 1.5 (K^+ and Na^+), a unique 001 reflection that corresponds to the same hydration state of the silicates is observed. In contrast, when the q/r ratio of the interlayer cations is higher than 1.5 (Li^+, Mg^{+2}, and Al^{+3}), a more complex behavior, with additional 001 reflections at high basal space, is observed. These data are consistent with the DTA/TG analysis results, where only one endothermic peak is observed when the q/r ratio is less than 1.5 and the number of water molecules obtained is similar in all cases. In contrast, several endothermic peaks are observed for higher q/r values, thus revealing the presence of different types of water molecules linked to the mica structure, which may be the cause of the new 001 reflection that appears in the diffractograms.

^{1}H MAS NMR

Structural information regarding the interlayer space of the silicates can be extracted from the ^{1}H MAS-NMR spectra of the hydrated silicate. In general, the ^{1}H NMR spectra of hydrated 2:1 phyllosilicates show two contributions: one due to interlayer water and the other due to hydroxyl groups (Alba et al., 2000). In this work, we will focus on analysis of the water contribution (signal at higher frequency). The chemical shifts obtained upon

deconvolution of all the ^{1}H spectra are plotted versus the pK_a value of the cations in aqueous solution (Figure 3, left) and versus the layer charge (Figure 3, right).

The analysis of ^{1}H data provide information about the Brönsted acidity, in the way that as the acidity of the site increases, the ^{1}H signal shifts to higher frequency (Pfeifer et al., 1991). Alba et al. (2000) have previously reported that proton shielding in smectites is related to the acidity of the cations in solution, as given by the pK_a value, although modulated by the total layer and the origin of the layer deficit. For all X-Mica-n samples, the ^{1}H water signal shifts toward lower frequencies as pK_a increases (Figure 3, left), although the expected linear behavior is not observed. The main reason for this may be the influence of the layer charge in the local environment of the protons. This influence of the layer charge on the local ordering of protons is examined in Figure 3 (right), where the ^{1}H chemical shifts for all the samples are plotted against the layer charge of the silicates. This figure shows a linear behavior for all samples, with a characteristic slope and intercept for each cation. In the case of Na^+ and Al^{+3}, the chemical shift increases proportionally to the charge, as expected in light of the increasing interlayer cation concentration, which results in an increased acidity (Alba et al., 2000). The fact that the other three cations (Li^+, K^+, and Mg^{+2}) behave oppositely suggests a high participation of an inner-sphere complex of these cations such that the coordination sphere of the interlayer cations is compensated by the basal oxygens, thereby decreasing the positive charge of the cations and, hence, their acidity (Alba et al., 2000).

Taken as a whole, these findings suggest that both the properties of the interlayer cations (such as acidity) and the layer charge of the silicate are responsible for the proton shielding experienced by the interlayer water in the presence of a high electric field such as that found in the interlayer space of the highly charged micas studied herein (Alba et al., 2003).

CONCLUSIONS

For the first time, the hydration property of a set of high-charge mica samples with a layer charge of between 2 and 4 and with different hydrated interlayer cations has been analyzed. The X-ray diffraction analysis and thermogravimetric results have shown that the hydration state depends on both the layer charge and the nature of the interlayer cation. Similarly, the thermogravimetric results show a low coordination number for the hydrated interlayer cations, whose coordination sphere is completed by the basal oxygen of the tetrahedral layer of the silicates. This high participation of inner-sphere complexes in a confined space with a high electric charge, such as the interlayer space, induces a much higher Brönsted acidity for the solid than would be expected for these cations in solution. In light of this, novel materials with appropriate Brönsted acidity could be synthesized by choosing the appropriate combination of interlayer cation and layer charge of the highly charged expandable mica.

ACKNOWLEDGMENTS

We gratefully acknowledge financial support from the DGICYT (project no. CTQ2010-14874) and FEDER funds. We would also like to thank the X-ray laboratory at CITIUS (Universidad de Sevilla) for its help recording the XRD patterns.

REFERENCES CITED

Adams, J.M. (1987) Synthetic organic chemistry using pillared, cation-exchanged and acid-treated montmorillonite catalysts - A review. Appl. Clay Sci., 2, 309–342.

Alba, M.D., Becerro, A.I., Castro, M.A. and Perdigon, A.C. (2000) High-resolution ^{1}H MAS NMR spectra of 2:1 phyllosilicates. Chem. Comm., 1, 37–38.

——— (2001) Hydrothermal reactivity of Lu-saturated smectites: Part I. A long-range order study. Am. Min., 86, 115-123.

Alba, M.D., Becerro, A.I., Castro, M.A., Perdigon, A.C. and Trillo, J.M. (2003) Inherent acidity of aqua metal ions in solids: An assay in layered aluminosilicates. J. Phys. Chem. B, 107, 3996–4001.

Alba, M.D., Castro, M.A., Naranjo, M. and Pavon, E. (2006) Hydrothermal reactivity of Na-n-micas (n = 2, 3, 4). Chem. Mat., 18, 2867-2872.

Alba, M.D., Castro, M.A., Orta, M.M., Pavón, E., Pazos, C. and Valencia, J. (2011) Formation of organo-highly charged mica. Langmuir, 27, 9711-9718.

Balek, Van O. (1997) An Introduction to Clay Colloid Chemistry, 2nd Edition. Wiley, New York.

Balek, Van O., Benes, M., Subrt, J., Pérez-Rodriguez, J.L., Sanchez-Jimenez, P.E., Perez-Maqueda, L.A. and Pascual-Cosp, J. (2008). Thermal characterization of montmorillonite clays saturated with various cations. J. Therm. Anal. Cal., 92, 191-197.

Barrer, R. M., Ward, D. J. and Rees, L. V. C. (1963) Thermochemistry and thermodynamics of ion exchange in a crystalline exchange medium. Proc. R. Soc. London, 273, 180–197.

Bérend, I., Cases , J. M., Francois, M., Uriot , J.P., Michot, L.J., Masion, A. and Thomas, F. (1995) Mechanism of adsorption and desorption of water vapour by homoionic montmorillonite 2. The Li^+, Na^+, K^+ etc. exchanged forms. Clay Clay Miner., 43, 324–336.

Bergaya, F., Theng, B.G.K. and Lagaly, G. (2006) Handbook of Clay Science. Elsevier, Amsterdam.

Boek, E.S., Coveney, P.V. and Skipper, N.T. (1995a) Molecular modeling of clay hydration: a study of hysteresis loops in the swelling curves of sodium montmorillonites. Langmuir, 11, 4629–4631.

——— (1995b) Monte Carlo molecular modelling studies of hydrated Li-, Na- and K smectites: understanding the role of potassium as a clay swelling inhibitor. J. Am. Chem. Soc., 117, 12608–12617.

Cases, J. M., Bérend, I., Francois, M., Uriot, J.P., Thomas, F. and Poirier, J.E. (1992) Mechanism of adsorption and desorption of water vapour by homoionic montmorillonite 1. The sodium exchanged form. Langmuir, 8, 2730–2739.

Chiou, C.T. and Rutherford, D.W. (1997) Effects of exchanged cation and layer charge on the sorption of water and EGME vapors on montmorillonite clays, Clays Clay Miner., 45, 867-880.

Colin, C.H. and Murray, H.H. (1997) Industrial clays in the 21st century: A perspective of exploration, technology and utilization. Appl. Clay Sci., 11, 285–310.

Criscenti, L.J. and Sverjensky, D.A. (1999). The role of electrolyte anions (ClO_4^-, NO_3^-, and Cl^-) in divalent metal (M^{2+}) adsorption on oxide and hydroxide surfaces in salt solutions. Am. J. Sci., 299, 828–899.

de Siqueira, A.V.C., Skipper, N.T., Coveney, P.V. and Boek, E.S. (1997) Computer simulation evidence for enthalpy driven dehydration of smectite clays at elevated pressures and temperatures. Mol. Phys., 92, 1–6.

Dyer, A., Chow, J.K.K. and Umar, I.M. (2000). The uptake of caesium and strontium radioisotopes onto clays. J. Mater. Chem., 10, 2734–2740.

Dysthe, D. K. and Wogelius, R. A. (2006) Physics and chemistry of confined fluids. Chem. Geol., 230, 175–242.

Eisenmann, G. (1962) Cation selective glass electrodes and their mode of operation. Biophys. J., 2, 259–323.

Ewin, G.J., Erno, B.P. and Hepler, L.G. (1981) Clay chemistry investigation of thermodynamics of ion-exchange reactions by titration calorimetry. Can. J. Chem., 59, 2927–2933.

Ferrage, E., Lanson, B., Malikova, N., Plancon, A., Sakharov, B.A. and Drits, V. A. (2005) New insights on the distribution of interlayer water in bi-hydrated smectite from X-ray diffraction profile modeling of 00l reflections. Chem. Mater., 17, 3499–3512.

Ferrage, E., Lanson, B., Sakharov, B.A. and Drits, V.A. (2005) Investigation of smectite hydration properties by modeling experimental X-ray diffraction patterns: Part I: Montmorillonite hydration properties. Am. Miner., 90, 1358-1374.

Finney, J.L (2001) The water molecule and its interactions: the interaction between theory, modeling and experiment. J. Mol. Liq., 90, 303-312.

Fripiat, J., Cloos, P. and Poncelet, A. (1964) Comparaison entre les propriétés d'échange de la montmorillonite et d'une résine vis-à-vis des cations alcalins et alcalino-terreux I. réversibilité des processus. Bull. Soc. Chim. Fr., 1, 208–221.

Gast, R. G. (1969) Standard free energy of exchange for alkali metal cations on wyoming bentonite. Soil Sci. Soc. Am. J., 33, 37–41.

——— (1992) Alkali metal cation exchange on chambers montmorillonite. Soil Sci. Soc. Am. J., 36, 14–19.

Glasser, R.I., Mantin, I. and Mering, J. (1960) Intern. Geol. Congr. 21st Session, Norden, France, pp. 28–34.

Gregorkiewitz, M. and Rausell-Colom, J. A. (1987) Characterization and properties of a new synthetic silicate with highly charged mica-type layers. Am. Miner., 72, 515-527.

Grim, R. E. (1942) Modern Concepts of Clay Materials. J. Geology, 50, 225-275.

——— (1962) Applied Clay Mineralogy. McGraw-Hill, New York.

Hardward, M.E., Carstea, D.D. and Sayegh, A.H. (1969) Properties of vermiculites and smectites: Expansion and collapse. Clays Clay Miner., 16, 437-447

Hendricks, S. B. and Jefferson, M. E. (1938) Structures of kaolin and talc-pyrophyllite hydrates and their bearing on water sorption of the clays. Am. Miner., 23, 863-875.

Hendricks, S.B., Nelson, R.A. and Alexander, L.T. (1940) Hydration Mechanism of the Clay Mineral Montmorillonite Saturated with Various Cations. J. Amer. Chem. Soc., 62, 1457-1464.

Hensen, E.J.M., Tambach, T.J., Bliek, A. and Smit, B. (2001) Adsorption isotherms of water in Li-, Na-, and K-montmorillonite by molecular simulation. J. Chem. Phys, 115, 3322-3329.

Hensen, E. J. M. and Smit, B. (2002) Why clays swell. J. Phys. Chem. B, 106, 12664–12667.

Jepson, W.B. (1984) Kaolins: their properties and uses. Philosophical Transactions of the Royal Society of London, 311, 411–432.

Justo, A., Pérez-Rodríguez, J.L. and Sánchez-Soto, P.J. (1993) Thermal study of vermiculites and mica-vermiculite interstratifications. J. Therm. Anal., 40, 59-65.

Kittrick, J.A. (1969) Interlayer Forces in Montmorillonite and Vermiculite. Soil Sci. Soc. Am. Proc., 33, 217-222.

——— (1969) Hydration of Layer Silicate Surfaces and Exchangeable Cations. Soil Sci. Soc. Am. Proc., 33, 980-980.

Komarneni, S., Ravella, R. and Park, M. (2005) Swelling mica-type clays: Synthesis by NaCl melt method, NMR characterization and cation exchange selectivity. J. Mater. Chem., 15, 4241-4245.

Laird, D.A. (1996) Model for crystalline swelling of 2:1 phyllosilicates. Clay Clay Miner., 44, 553-559.

——— (1999) Layer charge influences on the hydration of expandable 2:1 phyllosilicates. Clay Clay Miner., 47, 630-636.

Laird, D. A. and Shang, C. (1997) Relationship between cation exchange selectivity and crystalline swelling in 2:1 expanding phyllosilicates. Clay Clay Miner., 45, 681–689.

Lambert, J.-F., Poncelet, G., 1997. Acidity in pillared clays: origin and catalytic manifestations. Topics in Catalysis 4, 43–56.

Laszlo, P. (1986) Catalysis of organic reactions by inorganic solids. Acc. Chem. Res., 19,121–127.

Liu, X.D. and Lu, X.C. (2006) A thermodynamic understanding of clay-swelling inhibition by potassium ions. Angew. Chem. Int. Ed., 45, 6300–6303.

Mackenzie, R.C. (1964) Hydrationseigenschaften von Montmorillonit. Ber. Deut. Keram. Ges., 41, 696-708.

Maes, A. and Cremers, A. (1978) Charge density effects in ion exchange. Part 2. Homovalent exchange equilibria. J. Chem. Soc. Faraday Trans., 74, 1234–1241.

——— (1986) Highly selective ion exchanger in clay minerals and zeolites. In Geochemical Processes at Mineral Surfaces (eds. J. A. David and K. F. Hayes). American Chemical Society, Washington DC, pp. 254–295.

Martin, H. and Laudelout, H. (1963) Thermodynamique de l'échange des cations alcalins dans les argiles. J. Chim. Phys., 60, 1086–1099.

Melkior, T., Gaucher, E.C., Brouard, C., Yahiaoui, S., Thoby, D., Clinard, C., Ferrage, E., Guyonnet, D., Tournassat, C. and Coelho, D. (2009) Na^+ and HTO diffusion in compacted bentonite: Effect of surface chemistry and related texture. J. Hydr., 370, 9-20.

Menes, M., Málek , Z., Matuschek, G., Kettrup, A. and Yariv, S. (2006) Emanation thermal analysis study of Na-montmorillonite and montmorillonite saturated with various cations. J. Therm. Anal. Cal., 83, 617-623.

Michalopoulos, P. and Aller, R. C. (1995) Rapid clay mineral formation in Amazon delta sediments: Reverse weathering and oceanic elemental cycles. Science, 270, 614–617.

Michot, L.J., Villiéras F., Francois M., Bihannic I., Pelletier, M. and Cases, J. M. (2002) Water organisation at the solid-aqueous solution interface. C. R. Geosciences, 334, 611–631.

Michot, L.J., Bihannic, I., Pelletier, M., Rinnert, E. and Robert, J.L. (2005) Hydration and swelling of synthetic Na-saponites: Influence of layer charge. Am. Miner., 90, 166-172.

Miller, S.E., Heath, G.R., and González, R.D. (1982) Effects of Temperature on the Sorption of Lanthanides by Montmorillonites. Clays and Clay Minerals, 30, 111–122.

Mooney, R.W., Keenan, A.G and Wood, L.A. (1952a) Adsorption of water vapor by montmorillonite. I. Heat of desorption and application of BET theory. J. Am Chem Soc., 74, 1367-1371.

——— (1952b) Adsorption of water vapor by montmorillonite. II. Effect of exchangeable ions and lattice swelling as measured by X-ray diffraction. *J. Am Chem Soc* **74**, 1371-1374.

Murray, H.H. editor. (1986) Clays in: Ullmann's Encyclopedia of Industrial Chemistry. Wiley-VCH Verlag GmbH & Co. KGaA, Weinheim, Germany.

——— (1999) Applied clay mineralogy today and tomorrow. Clay Min., 34, 39–49.

——— (2000) Traditional and new applications for kaolin, smectite, and palygorskite: A general overview. Appl. Clay Sci., 17, 207–221.

Norrish, K. (1954) Crystalline swelling of montmorillonite: Manner of swelling of montmorillonite. Nature, 173, 256-257.

Odom, I.E. (1984) Smectite clay minerals: properties and uses. Philosophical Transactions of the Royal Society of London, A311, 391–409.

Park, M., Lee, D.H., Choi, C.L., Kim, S.S., Kim, K.S. and Choi, J. (2002) Pure Na-4-mica: Synthesis and Characterization. Chem. Mater., 14, 2582-2589.

Pfeifer, H. (1988) Highly resolved solid-state proton magnetic-resonance studies of zeolites. J. Chem. Soc., Faraday Trans. I, 84, 3777-3783.

Ravella, R.; Komarneni, S. and Martinez, C.E. (2008) Highly charged swelling mica-type clays for selective Cu exchange. Env. Sci. Tech., 42, 113-118.

Rayner-Canham, A.G. (2000) Química Inorgánica Descriptiva. Ed. Pearson Education, México, pp 182-183.

Rinnert, E., Carteret, C., Humbert, B., Fragneto-Cusani, G., Ramsay, J.D.F., Delville, A., Robert, J.L., Bihannic, I., Pelletier, M. and Michot, L.J. (2005) Hydration of a synthetic clay with tetrahedral charges: a multidisciplinary experimental and numerical study. J. Phys. Chem. B, 109, 23745–23759.

Robeyns, J., van Bladel, R. and Laudelout, H. (1971) Thermodynamics of singly charged ion exchanges in trace regions on Camp Berteau montmorillonite. J. Soil Sci., 22, 336–341.

Salles, F., Beurroies, I., Bildstein, O., Jullien, M., Raynal, J., Denoyel, R. and Van Damme, H. (2008) A calorimetric study of mesoscopic swelling and hydration sequence in solid Namontmorillonite. Appl. Clay Sci., 39, 186–201.

Sato, T., Watanabe, T. and Otsuka, R. (1992) Effects of layer charge, charge location, and energy change on expansion properties of dioctahedral smectites. Clay Clay Miner., 40, 103-113.

Shainberg, I. and Kemper, W. D. (1967) Ion exchange equilibria on montmorillonite. Soil Sci., 103, 4–9.

Slabaugh, W.H. (1954) Cation exchange properties of bentonite. J. Phys. Chem., 58, 162–165.

Slade, P.G., Quirk, J.P. and Norrish, K. (1991) Crystalline swelling of smectite samples in concentrated NaCl solutions in relation to layer change. Clay Clay Miner., 39, 234-238.

Smith, D.E., Wang, Y., Chaturvedi, A. and Whitley, H.D. (2006) Molecular simulations, of the pressure, temperature, and chemical potential dependencies of clay swelling. J. Phys. Chem. B, 110, 20046–20054.

Sposito, G. (1984) The Surface Chemistry of Soils. Oxford University Press.

——— (1989) The Chemistry of Soils. Oxford University Press, New York, USA.

Sposito, G. and Prost, R. (1982) Structure of water adsorbed on smectites. Chem. Rev., 82, 553-573.

Sposito, G., Skipper, N., Sutton, R., Park, S.H., Soper, A. and Greathouse, F. (1999) Surface geochemistry of the clay minerals. Proc. Nat. Academy of Sciences of the United States of America, 96, 3358–3364.

Srodon, J. (1980) Precise identification of illite/smectite interstratifications by X-ray powder diffraction. Clays Clay Min., 28, 401–411.

——— (2006) Indentification and quantitative analysis of clay minerals. Chapter 12.2. in Handbook of Clay Science. Edited by F. Bergaya, B.K.G. Theng and G. Lagaly. Developments in Clay Science, Vol. 1. Elsevier Ltd.

Tambach T. J., Bolhuis P. G. and Smit B. (2004) A molecular mechanism of hysteresis in clay swelling. Angew. Chem. Int. Ed., 43, 2650–2652.

Tambach, T.J., Bolhuis, P.G., Hensen, E.J.M. and Smit, B. (2006) Hysteresis in clay swelling induced by hydrogen bonding: accurate prediction of swelling states. Langmuir, 22, 1223–1234.

Trausch, G., Canet, D., Cadéne, A. and Turq, P. (2006) Separation of components of a ^{1}H NMR composite signal by nutation experiments under low amplitude radio-frequency fields. Application to the water signal in clays. Chem. Phys. Lett., 433, 228–233.

Van Olphen. (1977) An Introduction to Clay Colloid Chemistry, 2nd Edition. Wiley, New York.

Wang, Y.F., Bryan, C., Xu, H. F. and Gao, H. Z. (2003) Nanogeochemistry: geochemical reactions and mass transfers in nanopores. Geology, 31, 387–390.

Weiss, C. A., Kirkpatrick, R. J. and Altaner, S. P. (1990) Variations in interlayer cation sites of clay minerals as studied by ^{133}Cs MAS nuclear magnetic resonance spectroscopy. Am. Mineral., 75, 970–982.

Whitley, H.D. and Smith, D.E. (2004) Free energy, energy, and entropy of swelling in Cs-, Na-, and Sr-montmorillonite clays. J. Chem. Phys., 120, 5387–5395.

Yariv, S. (1992) Modern approach to wettability, M. A. Schrader and G. Loeb, Eds, Plenum Press, New York pp. 279–326.

Young, D.A. and Smith, D.E. (2000) Simulations of clay mineral swelling and hydration: Dependence upon interlayer ion size and charge. J. Phys. Chem. B, 104, 9163–9170.

TABLE 1. Physicochemical properties of cations. *r* represents the Pauling ionic radius, *q/r* is the relation between the ionic charge and ionic radius. ΔH^{o}_{hyd} is the hydration enthalpy and pK_a is the acidity constant.

	K^{+}	Na^{+}	Li^{+}	Mg^{+2}	Al^{+3}
r (Å)	1.33	0.95	0.6	0.65	0.5
q/r	0.75	1.05	1.70	3.08	6.00
ΔH^{o}_{hyd}(KJ/mol)	-305	-406	-519	-1922	-4660
pK_a	14.5	14.2	13.6	11.4	5.0

TABLE 2. Temperatures of the main endothermic peaks observed in the DTA for all the samples X- Mica-*n* and number of water molecules per unit cell calculated using the TG.

	Li^{+}		Na^{+}		K^{+}		Mg^{+2}		Al^{+3}	
	T (ºC)	nº H_2O/u.c	T (ºC)	nº H_2O/u.c	T (ºC)	nº H_2O/u.c	T (ºC)	nº H_2O/u.c	T (ºC)	nº H_2O/u.c
n=4	86.27	2.86	69.47	3.14	66.61	2.92	69.95	3.17	65.73 140.80	1.85
n=3	85.05 145.49	3.33	72.56	2.54	63.34	2.03	80.47 139.68 198.4	5.01	62.20 89.76 186.3	6.53
n=2	83.08 158.55	3.74	66.93	2.30	62.94	2.15	76.63 156.77 194.9	5.96	64.2 112.76 183.72	5.04

FIGURE CAPTION

FIGURE 1. Number of water molecules per cation versus the ionic radius (a), and, versus the factor q/r of the third period cations (b) for the mica homoionized with the alkaline cations.

FIGURE 2. 001 reflection obtained by oriented aggregated in water of a) X-Mica-2, b) X-Mica-3, and, c) X-Mica-4. X=Li, Na, K, Mg and Al.

FIGURE 3. ^{1}H NMR chemical shifts value of the water resonance peak as a function of a) acidity constant of the cations in solutions, and, b) lager charge.

Figure 1

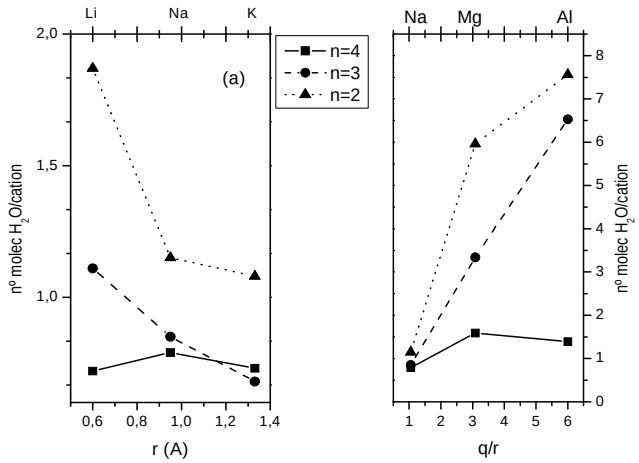

Figure 2

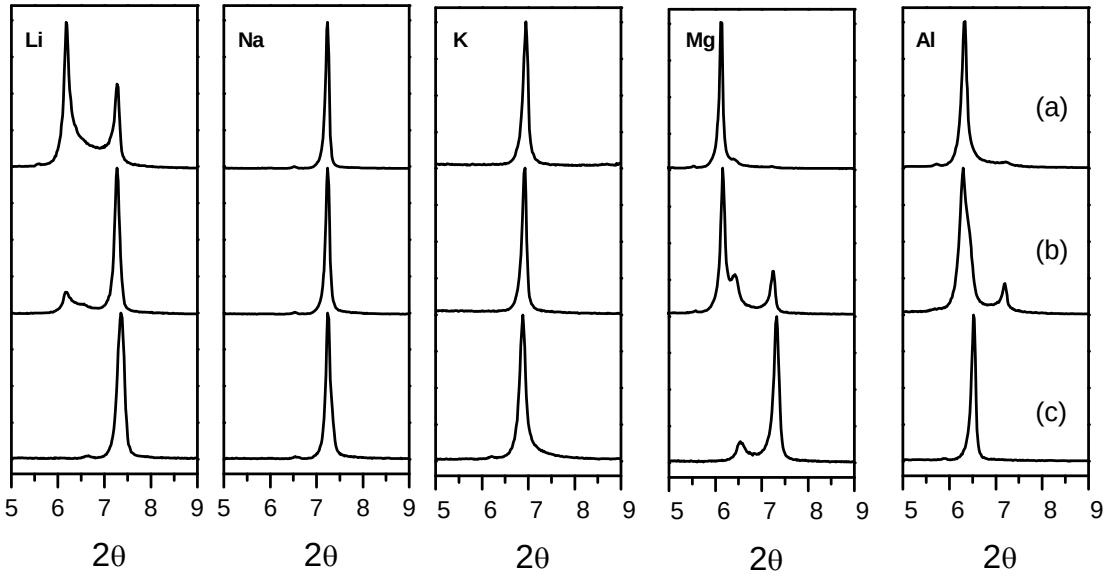

Figure 3